

NASA TECHNICAL NOTE



NASA TN D-6181

C.1

NASA TN D-6181

LOAN COPY: RETURN TO
AFWL (DOCUMENTS)
KIRTLAND AFB



EFFECT OF VELOCITY SLIP AT
A POROUS BOUNDARY ON THE PERFORMANCE
OF AN INCOMPRESSIBLE POROUS BEARING

by Marvin E. Goldstein and Willis H. Braun

*Lewis Research Center
Cleveland, Ohio 44135*



0133234

1. Report No. NASA TN D-6181		2. Government Accession No.		3. Recipient's Catalog No.	
4. Title and Subtitle EFFECT OF VELOCITY SLIP AT A POROUS BOUNDARY ON THE PERFORMANCE OF AN INCOMPRESSIBLE POROUS BEARING				5. Report Date February 1971	
				6. Performing Organization Code	
7. Author(s) Marvin E. Goldstein and Willis H. Braun				8. Performing Organization Report No. E-5906	
9. Performing Organization Name and Address Lewis Research Center National Aeronautics and Space Administration Cleveland, Ohio 44135				10. Work Unit No. 129-01	
				11. Contract or Grant No.	
12. Sponsoring Agency Name and Address National Aeronautics and Space Administration Washington, D.C. 20546				13. Type of Report and Period Covered Technical Note	
				14. Sponsoring Agency Code	
15. Supplementary Notes					
16. Abstract There is an effective slip in velocity of a fluid flowing over a porous surface. The effect of this slip on the performance of a porous bearing is established by obtaining solutions for the short bearing limit. The slip has a significant effect on bearing performance of small, high-speed, low-load bearings. A simple correction is given to the bearing friction formula to take into account the effects of slip.					
17. Key Words (Suggested by Author(s)) Journal bearings Porous media Reynolds equation			18. Distribution Statement Unclassified - unlimited		
19. Security Classif. (of this report) Unclassified		20. Security Classif. (of this page) Unclassified		21. No. of Pages 36	22. Price* \$3.00

EFFECT OF VELOCITY SLIP AT A POROUS BOUNDARY ON THE
PERFORMANCE OF AN INCOMPRESSIBLE POROUS BEARING

by Marvin E. Goldstein and Willis H. Braun

Lewis Research Center

SUMMARY

There is an effective slip in velocity of fluid flowing over a porous surface. The effect of this slip on the performance of a porous bearing is established by obtaining solutions for the short bearing limit. The slip has a significant effect on bearing performance of small, high-speed, low-load bearings. Other things being equal, the slip effects usually reduce both the load-carrying capability and the coefficient of friction of the bearing. For the larger eccentricity ratios this reduction in the coefficient of friction can be very large. The reduction in the load-carrying capability can be as much as 30 percent. However, the slip has little effect on the attitude angle. A simple correction is given to the bearing friction formula to take into account the effects of slip.

INTRODUCTION

Porous metal bearings have proved so practical for many applications that they are produced at the rate of about 20 million a day (ref. 1). The low initial cost of such bearings, combined with the design simplicity which they provide, has made them popular for aircraft and automotive accessories, home appliances, small motors, business machines, instruments, and farm and construction equipment. These bearings are available in thousands of sizes for shafts ranging from $1/32$ to 6 inches in diameter and with lengths varying from $1/32$ to 4 inches.

Most porous metal bearings are made of either bronze or iron with interconnecting pores. The porosity ranges from about 10 to 40 percent and for the majority of applications a porosity from 25 to 35 percent is used (ref. 2).

High-porosity bearings are used for high-speed, light-load applications, such as fractional-horsepower motor bearings. The low-porosity bearings are more satisfactory for applications where oscillating and reciprocating motions occur and it is

difficult to build up an oil film.

We shall be concerned in this report with the highly porous bearings which are operated with a hydrodynamic film. The first analysis of bearings of this type was performed by Morgan and Cameron in reference 2. In that paper the short-bearing approximation (ref. 3) was used and one additional approximation (discussed subsequently) was introduced. More recently Rouleau (ref. 4) corrected Morgan and Cameron's analysis by including a load component which had been neglected and recalculating the coefficient of friction on the basis of total load and actual eccentricity and attitude angle. In a second paper (ref. 5) Rouleau removed the additional restriction imposed by Morgan and Cameron with a considerable increase in the complexity of the analysis. The results of this analysis show that for those bearing configurations which occur in the majority of applications the approximation used by Morgan and Cameron leads to only an insignificant error (see remarks by discussors appended to ref. 5). Rhodes and Rouleau (ref. 6) analyzed the effect of sealing off the ends of a short bearing and found that the load could be increased.

Shir and Joseph (refs. 7 and 8) analyzed the infinitely long porous bearing. The principal difficulty with their analysis is that they assumed that the hydrodynamic film extends the full 360° around the bearing (full Sommerfeld condition) thus allowing large negative pressure regions in the film. This almost never occurs for bearings under the usual operating conditions. The finite partial porous bearing was analyzed in reference 9 by Rhodes and Rouleau. They also assumed that the hydrodynamic film extends around the entire bearing; but since the largest bearing arc which they considered was 180° , this was not a bad assumption. Finally, the porous gas-lubricated bearing was analyzed in a series of three papers by Sneck, Yen, and Elwell (refs. 10 to 12).

In all the analyses described in the preceding paragraphs, it was assumed that the tangential velocity in the film vanishes at the porous bearing surface. However, it was proved experimentally by Beavers and Joseph in reference 13 that, when a fluid flows over a porous wall, the tangential velocity does not vanish at the boundary but satisfies some sort of slip condition. A particular model for the slip condition was proposed, but the experiments performed in that study were not accurate enough to verify the model or to determine the empirical slip coefficient which appeared in the model. However, very accurate experiments were reported in a very recent paper by Beavers, Sparrow, and Magnuson (ref. 14) which did indeed verify the model proposed in reference 13 and determined for one porous material the value of the slip coefficient.

In the present report we shall study the effect of the slip at the porous metal surface on the performance of porous metal bearings. In the first section the general porous bearing problem is formulated (for the full bearing) and the generalized Reynolds' equation for porous bearings with the effects of slip included is derived. The short-bearing approximation is then made, and the approximation introduced by Morgan and Cameron

is then adapted to obtain a closed-form solution. The effects of slip introduce two additional parameters into the problem. The results show that for the values of the parameters corresponding to small bearings operated at high speeds and light loads the slip can have a significant effect on the bearing performance.

ANALYSIS

Formulation

Figure 1 shows a solid journal running in a cylindrical porous bearing of inside radius r_0 , outside radius r_1 and length l . The bearing is mounted in a solid housing, as shown in the figure. We suppose that the film region and the pores of the bearing are completely filled with an incompressible Newtonian fluid of constant viscosity η and that the assumptions of conventional lubrication theory apply to the flow within the film. Thus, it is assumed that the film is so thin that the motion of the fluid is laminar, the inertial terms and the curvature can be neglected, and the pressure p is uniform across the film. Therefore, if x is the coordinate measured along the inner bearing surface (with $x = 0$ at the point of maximum film thickness) in the circumferential direction, z is the coordinate measured along this surface in the axial direction (with $z = 0$ at the center of the bearing) and y is the coordinate normal to this surface, as shown in figure 2, and if the velocity components in these directions of the fluid film region are u , v , and w , respectively, then the Navier-Stokes equations become

$$\frac{\partial^2 u}{\partial y^2} = \frac{1}{\eta} \frac{\partial p}{\partial x} \quad (1)$$

$$\frac{\partial^2 v}{\partial y^2} = \frac{1}{\eta} \frac{\partial p}{\partial z} \quad (2)$$

$$\frac{\partial p}{\partial y} = 0 \quad (3)$$

The integrated volume fluxes in the x - and z -directions in the film, q_x and q_z , respectively, are defined by

$$q_x = \int_0^{h(x)} u(x, y, z) dy \quad (4)$$

$$q_z = \int_0^{h(x)} v(x, y, z) dy \quad (5)$$

where $h(x)$ is the local film thickness shown in figure 2. The integrated continuity equation for the film (ref. 15, p. 60) can now be written as

$$\frac{\partial q_x}{\partial x} + \frac{\partial q_z}{\partial z} = w(x, 0, z) \quad (6)$$

Suppose then the porous material is homogeneous and isotropic. Let \bar{Q} be the Darcy velocity (flow divided by total cross-sectional area, not just open area), let P denote the pressure within the porous region, and let κ denote the permeability of the bearing material. Then

$$\bar{Q} = -\frac{\kappa}{\eta} \nabla P \quad (7)$$

and conservation of mass implies that

$$\nabla \cdot \bar{Q} = 0 \quad (8)$$

Let r and θ be the polar coordinates shown in figure 1. The angle θ is measured from the position of maximum film thickness. Then, the r , θ , and z components of the Darcy velocity \bar{Q} are denoted by V_r , V_θ , and V_z , respectively. It is necessary to obtain the conditions which match the flow in the porous bearing to the flow in the film region. To this end notice that figures 1 and 2 show

$$x = r_0 \theta \quad (9)$$

Since the pressure and (from continuity) the normal component of the velocity must be continuous across the boundary of the porous bearing, it follows (in view of eq. (3)) that

$$\left. \begin{aligned} p(x, z) &= P(r_0, \theta, z) \\ w(x, 0, z) &= -V_r(r_0, \theta, z) \end{aligned} \right\} \begin{aligned} 0 &\leq \theta < 2\pi \\ -l/2 &\leq z \leq l/2 \end{aligned} \quad (10)$$

In addition to these conditions it is necessary to impose a condition on the tangential velocity at the bearing. In all previous work on porous bearings it has been assumed that the tangential film velocity vanishes at the surface of the porous bearing (refs. 2,

and 4 to 12). However, it has been shown in references 13 and 14 that in reality the tangential velocity components satisfy the following slip conditions at the bearing surface:

$$\left. \begin{aligned} \frac{\alpha}{\sqrt{k}} [u(x, 0, z) - V_{\theta}(r_0, \theta, z)] &= \frac{\partial u}{\partial y} \Big|_{y=0} \\ \frac{\alpha}{\sqrt{k}} [v(x, 0, z) - V_z(r_0, \theta, z)] &= \frac{\partial v}{\partial y} \Big|_{y=0} \end{aligned} \right\} \begin{aligned} 0 \leq \theta < 2\pi \\ -\frac{l}{2} \leq z \leq \frac{l}{2} \end{aligned} \quad (11)$$

where α is an effective slip coefficient. Notice that when $\kappa \rightarrow 0$ these boundary conditions, together with Darcy's law (eq. (7)), imply that $u(x, 0, z) = v(x, 0, z) = 0$, which is the no-slip boundary condition used in previous analyses. On the other hand these conditions also imply that $u(x, 0, z) = v_{\theta}(r_0, \theta, z)$ and $v(x, 0, z) = V_z(r_0, \theta, z)$ when $\alpha \rightarrow \infty$. It has been shown in reference 13 that α is probably a property of the porous material and does not depend on the type of fluid which is flowing through it. The experiments performed in reference 13 were not accurate enough to determine α . However, the experiments described in reference 14 show that for Foametal (General Electric Company) the value of α is 1/10.

The remaining boundary conditions for the flow in the film region follow from the no-slip condition at the shaft surface and the requirement that the pressure in the film be equal to zero at the ends of the bearing. Thus, if u_s is the surface speed of the shaft then

$$\left. \begin{aligned} u[x, h(x), z] &= u_s \\ v[x, h(x), z] &= 0 \end{aligned} \right\} \begin{aligned} -\frac{l}{2} \leq z \leq \frac{l}{2} \\ 0 \leq x \leq 2\pi r_0 \end{aligned} \quad (12)$$

and (since the ends of the bearing are open) the vanishing of the pressure curve at the ends of the bearing implies that

$$p\left(x, \frac{l}{2}\right) = p\left(x, -\frac{l}{2}\right) = 0 \quad \text{for} \quad 0 \leq x \leq 2\pi r_0 \quad (13)$$

Two additional boundary conditions are needed to determine the flow in the porous region. The first of these follows from the fact that the bearing is mounted in a solid housing. Hence,

$$V_r(r_1, \theta, z) = 0 \quad \left\{ \begin{array}{l} 0 \leq \theta \leq 2\pi \\ -\frac{l}{2} \leq z \leq \frac{l}{2} \end{array} \right. \quad (14)$$

The remaining boundary condition depends on the nature of the ends of the porous bearing. If the ends of the bearing are open to the atmosphere, then this boundary condition is

$$P\left(r, \theta, \frac{l}{2}\right) = P\left(r, \theta, -\frac{l}{2}\right) = 0 \quad \left\{ \begin{array}{l} r_0 \leq r \leq r_1 \\ 0 \leq \theta \leq 2\pi \end{array} \right. \quad (15a)$$

If the ends of the bearing are closed off, then the boundary condition is

$$V_z\left(r, \theta, \frac{l}{2}\right) = V_z\left(r, \theta, -\frac{l}{2}\right) = 0 \quad \left\{ \begin{array}{l} r_0 \leq r \leq r_1 \\ 0 \leq \theta \leq 2\pi \end{array} \right. \quad (15b)$$

Finally, the usual small clearance approximation for the film thickness

$$h = c + e \cos \theta \quad (16)$$

where c is the concentric clearance and e is the eccentricity (see fig. 1), is valid in the present context.

Derivation of boundary-slip Reynolds equation. - Upon integrating equations (1) and (2) and using the boundary conditions (12) we obtain

$$\left. \begin{array}{l} u(x, y, z) = \frac{1}{\eta} \left[\frac{1}{2} \frac{\partial p}{\partial x} (y - h)^2 + (y - h)f \right] + u_s \frac{y}{h} \\ v(x, y, z) = \frac{1}{\eta} \left[\frac{1}{2} \frac{\partial p}{\partial z} (y - h)^2 + (y - h)g \right] \end{array} \right\} \quad (17)$$

where f and g are arbitrary functions of x and z which are to be determined from the slip conditions (11). In order to do this, notice that equation (7) shows

$$V_{\theta} = -\frac{\kappa}{\eta} \frac{1}{r} \frac{\partial P}{\partial \theta}$$

$$V_z = -\frac{\kappa}{\eta} \frac{\partial P}{\partial z}$$

Hence, equations (9) and (10) show that

$$\left. \begin{aligned} V_{\theta}(r_0, \theta, z) &= -\frac{\kappa}{\eta} \frac{\partial p}{\partial x} \\ V_z(r_0, \theta, z) &= -\frac{\kappa}{\eta} \frac{\partial p}{\partial z} \end{aligned} \right\} \quad (18)$$

Upon inserting equations (17) and (18) into condition (11) we find that the functions f and g are

$$f = \frac{1}{2} \frac{\partial p}{\partial x} h \left(1 + \frac{1}{3} \Xi_1 \right) - \frac{\eta u_s}{h} \Xi_0$$

$$g = \frac{1}{2} \frac{\partial p}{\partial z} h \left(1 + \frac{1}{3} \Xi_1 \right)$$

where we have put

$$\left. \begin{aligned} \Xi_0 &\equiv \frac{\frac{\sqrt{\kappa}}{\alpha}}{\frac{\sqrt{\kappa}}{\alpha} + h} \\ \Xi_1 &\equiv \frac{3 \left(2\kappa + \frac{\sqrt{\kappa}}{\alpha} h \right)}{h \left(\frac{\sqrt{\kappa}}{\alpha} + h \right)} \end{aligned} \right\} \quad (19)$$

Substitute these results into equations (17) and then substitute the result of this equations (4) and (5) to obtain the following expressions for the integrated components of the volume flux:

$$\left. \begin{aligned} q_x &= -\frac{h^3}{12\eta} \frac{\partial p}{\partial x} (1 + \Xi_1) + \frac{u_s h}{2} (1 + \Xi_0) \\ q_z &= -\frac{h^3}{12\eta} \frac{\partial p}{\partial z} (1 + \Xi_1) \end{aligned} \right\} \quad (20)$$

Notice (see ref. 15, p. 290, e.g.) that these reduce to the usual expressions for the fluxes in nonporous bearing when Ξ_1 and Ξ_0 are put equal to zero. If Ξ_1 and Ξ_0 are zero, these expressions would also apply to porous bearings if there were no slip at the surface of the porous bearing.

The expressions for the velocity distribution in the x -direction can also be used to obtain expressions for the shear stress τ_h acting on the shaft and the shear stress τ_0 acting on the bearing. Thus,

$$\tau_h = \eta \left. \frac{\partial u}{\partial y} \right|_{y=h} = \frac{1}{2} \frac{\partial p}{\partial x} h \left(1 + \frac{1}{3} \Xi_1 \right) + \frac{\eta u_s}{h} (1 - \Xi_0) \quad (21a)$$

$$\tau_0 = \eta \left. \frac{\partial u}{\partial y} \right|_{y=0} = +\frac{1}{2} \frac{\partial p}{\partial x} h \left(\frac{1}{3} \Xi_1 - 1 \right) + \frac{\eta u_s}{h} (1 - \Xi_0) \quad (21b)$$

In order to obtain the porous-bearing Reynold's equation, the second boundary condition (10) and equations (20) are first substituted into equation (6) to obtain

$$\frac{\partial}{\partial x} \left[\frac{h^3}{12\eta} \frac{\partial p}{\partial x} (1 + \Xi_1) \right] + \frac{\partial}{\partial z} \left[\frac{h^3}{12\eta} \frac{\partial p}{\partial z} (1 + \Xi_1) \right] = \frac{u_s}{2} \frac{\partial}{\partial x} \left[h(1 + \Xi_0) + V_r(r_0 \theta, z) \right]$$

On using equation (7)

$$\frac{\partial}{\partial x} \left[\frac{h^3}{\eta} \frac{\partial p}{\partial x} (1 + \Xi_1) \right] + \frac{\partial}{\partial z} \left[\frac{h^3}{\eta} \frac{\partial p}{\partial z} (1 + \Xi_1) \right] = 6u_s \frac{\partial}{\partial x} h(1 + \Xi_0) - \frac{12\kappa}{\eta} \frac{\partial P}{\partial r} \Big|_{r=r_0} \quad (22)$$

This is the appropriate form of Reynolds equation for porous bearings. Equation (24.10) on page 549 of reference 15 is the porous-bearing Reynolds equation when slip at the bearing interface is neglected. A comparison of these two equations shows that equation (22) reduces to the no-slip equation when Ξ_1 and Ξ_0 are put equal to zero. Thus, the effects of slip at the porous-bearing/liquid-film interface are accounted for by the

factors $\bar{\epsilon}_1$ and $\bar{\epsilon}_0$. The term $\left. \frac{\partial P}{\partial r} \right|_{r=r_0}$ in equation (22) connects the flow in the film region with the flow in the porous bearing. Hence, it is necessary to consider the equations for the flow in the porous region before the Reynolds equation (22) can be solved.

Mathematical description of the flow within the porous region. - When equation (7) is substituted into equation (8), we obtain the well-known result that the pressure within the porous region is governed by Laplace's equation. Thus,

$$\nabla^2 P = 0$$

which when written out in polar coordinates is

$$\frac{1}{r} \frac{\partial}{\partial r} \left(r \frac{\partial P}{\partial r} \right) + \frac{1}{r^2} \frac{\partial^2 P}{\partial \theta^2} + \frac{\partial^2 P}{\partial z^2} = 0 \quad (23)$$

It also follows from equation (7) that the boundary condition (14) is

$$\left. \frac{\partial P}{\partial r} \right|_{r=r_1} = 0 \quad \left\{ \begin{array}{l} 0 \leq \theta \leq 2\pi \\ -\frac{l}{2} \leq z \leq \frac{l}{2} \end{array} \right. \quad (24)$$

It follows from the first condition (10) and equation (9) that the Reynolds equation (22) provides the boundary condition for equation (23) on the surface $r = r_0$. The boundary conditions on the remaining surfaces are given either by equation (15a) or (15b). Thus, the pressure distribution in the bearing (and, in view of the first eq. (10), the pressure distribution in the film) is completely determined by equation (23) and these boundary conditions.

Nondimensional formulation. - Before proceeding it is convenient to introduce the following standard nondimensional quantities

$$\left. \begin{aligned}
 z^* &= \frac{z}{r_0} \\
 r^* &= \frac{r}{r_0} \\
 r_1^* &= \frac{r_1}{r_0} \\
 l^* &= \frac{l}{r_0} \\
 h^* &= \frac{h}{c} \\
 p^* &= \frac{pc^2}{6u_s \eta r_0} \\
 P^* &= \frac{Pc^2}{6u_s \eta r_0} \\
 \epsilon &= \frac{e}{c} \\
 \Psi &\equiv \frac{\kappa r_0}{c^3} \\
 s &\equiv \frac{\sqrt{\kappa}}{\alpha c}
 \end{aligned} \right\} \quad (25)$$

Then equations (16), (22), and (23) become, respectively,

$$h^* = 1 + \epsilon \cos \theta \quad (26)$$

$$\frac{\partial}{\partial \theta} \left[(h^*)^3 \frac{\partial p^*}{\partial \theta} (1 + \bar{\Xi}_1) \right] + \frac{\partial}{\partial z^*} \left[(h^*)^3 \frac{\partial p^*}{\partial z^*} (1 + \bar{\Xi}_1) \right] = \frac{d}{d\theta} [h^* (1 + \bar{\Xi}_0)] - 12\psi \left. \frac{\partial P^*}{\partial r^*} \right|_{r^*=1} \quad (27)$$

$$\frac{1}{r^*} \frac{\partial}{\partial r^*} \left(r^* \frac{\partial P^*}{\partial r^*} \right) + \frac{1}{r^{*2}} \frac{\partial^2 P^*}{\partial \theta^2} + \frac{\partial^2 P^*}{\partial z^{*2}} = 0 \quad (28)$$

where after using equation (16) the nondimensional slip terms $\bar{\Xi}_1$ and $\bar{\Xi}_0$ can now be written as

$$\bar{\Xi}_0 = \frac{s}{1 + s + \epsilon \cos \theta} \quad (29)$$

$$\bar{\Xi}_1 = \frac{3[2\alpha^2 s^2 + s(1 + \epsilon \cos \theta)]}{(1 + \epsilon \cos \theta)(s + 1 + \epsilon \cos \theta)} \quad (30)$$

The first condition (10) becomes

$$p^*(\theta, z^*) = P^*(1, \theta, z^*) \quad \begin{cases} 0 \leq \theta \leq 2\pi \\ -\frac{l^*}{2} \leq z^* \leq \frac{l^*}{2} \end{cases} \quad (31)$$

The boundary condition (24) becomes

$$\left. \frac{\partial P^*}{\partial r^*} \right|_{r^*=r_1^*} = 0 \quad \begin{cases} 0 \leq \theta \leq 2\pi \\ -\frac{l^*}{2} \leq z^* \leq \frac{l^*}{2} \end{cases} \quad (32)$$

We shall not consider the boundary condition (15b). The boundary conditions (13) and (15a) are, respectively,

$$p^* \left(\theta, \frac{l^*}{2} \right) = p^* \left(\theta, -\frac{l^*}{2} \right) = 0 \quad 0 \leq \theta < 2\pi \quad (33a)$$

$$P^* \left(r^*, \theta, \frac{l^*}{2} \right) = P^* \left(r^*, \theta, -\frac{l^*}{2} \right) = 0 \quad \begin{cases} 1 \leq r^* \leq r_1^* \\ 0 \leq \theta < 2\pi \end{cases} \quad (33b)$$

Notice that in view of condition (31) the boundary condition (33b) implies the boundary condition (33a) provided it is required that the pressure be continuous at the points $\left(1, \theta, \frac{l^*}{2} \right)$ and $\left(1, \theta, -\frac{l^*}{2} \right)$. (Notice that this would not be the case if the condition (15b) was imposed.) Hence, the boundary condition (33a) can be replaced by a pressure continuity condition. We shall use these boundary conditions in a somewhat different way and it is therefore convenient to retain them in their present form.

Equations (26) to (33b) completely determine the boundary value problem for the pressure distribution within the bearing and film region. Notice that the parameter s enters these equations only through the terms Ξ_0 and Ξ_1 and that Ξ_0 and Ξ_1 equal zero when s is equal to zero. Hence, the effect of the slip at the bearing surface goes to zero when s goes to zero.

Instead of obtaining the complete solution to the boundary value problem we shall consider the short-bearing approximation.

Short-bearing approximation. - The short-bearing approximation consists of assuming the pressure gradient in the circumferential direction is negligibly small compared with the pressure gradient in the axial direction (ref. 3). This assumption is usually valid for l/d ratios less than 1. Many porous bearings fall into this geometric category. When this approximation is made (since eqs. (26) and (30) show that h^* and Ξ_1 are independent of z^*), equations (27) and (28) become

$$(h^*)^3 (1 + \Xi_1) \frac{\partial^2 P^*}{\partial z^{*2}} + 12\Psi \frac{\partial P^*}{\partial r^*} \Big|_{r^*=1} = \frac{d}{d\theta} [h^* (1 + \Xi_0)] \quad (34)$$

$$\frac{1}{r^*} \frac{\partial}{\partial r^*} \left(r^* \frac{\partial P^*}{\partial r^*} \right) + \frac{\partial^2 P^*}{\partial z^{*2}} = 0 \quad (35)$$

These equations must be solved subject to the boundary conditions (32), (33a), and (33b). This boundary value problem has been solved exactly for the limiting case of zero slip in reference 5 in terms of infinite series. However, a much simpler approximate solution was obtained for this problem in the zero slip case by Morgan and Cameron in reference 2. It was pointed out by Pinkus in his discussion of reference 5 (appended to ref. 5) that for the values of the parameters which correspond to the majority of

bearings there is practically no difference between these solutions. We shall therefore simplify the problem by introducing the approximation of Morgan and Cameron. This approximation consists of imposing only the boundary condition (33a) and not the boundary condition (33b), and of using the arbitrariness introduced by this means to obtain a simple expression for the solution. This approximation is equivalent to imposing the boundary condition (33b) only along a single line at the edge of the bearing instead of over the entire edge. Since this line is adjacent to the film, this turns out to be a good approximation for the bearing geometries usually used in practice.

We shall, therefore, seek a solution to equation (35) subject to the conditions (31), (32), (33a), and (34). This problem possesses a solution of the form

$$P^*(r^*, \theta, z^*) = R(r^*, \theta) + Z(z^*, \theta) \quad (36)$$

where the functions R and Z can be determined so that all the conditions are satisfied. In order to prove this it is only necessary to find the functions R and Z which satisfy equation (35) together with conditions (31), (32), (33a), and (34). To this end, insert equation (36) into equation (35) to obtain

$$\frac{1}{r^*} \frac{\partial}{\partial r^*} \left(r^* \frac{\partial R}{\partial r^*} \right) = - \frac{\partial^2 Z}{\partial z^{*2}}$$

Since the left side of this equation is independent of z^* and the right side is independent of r^* , there exists a function Θ of θ only such that

$$\frac{1}{r^*} \frac{\partial}{\partial r^*} \left(r^* \frac{\partial R}{\partial r^*} \right) = \Theta(\theta)$$

$$\frac{\partial^2 Z}{\partial z^{*2}} = - \Theta(\theta)$$

Hence, upon carrying out the integrations, we find that

$$r^* \frac{\partial R}{\partial r^*} = \frac{1}{2} (r^*)^2 \Theta + \Theta_1(\theta) \quad (37)$$

And equation (35) will be satisfied provided

$$R = \frac{1}{4}(r^*)^2\Theta(\theta) + \ln r^* \Theta_1(\theta) + \Theta_2(\theta) \quad (38)$$

$$Z = -\frac{1}{2}(z^*)^2\Theta(\theta) + \Theta_3(\theta)z^* + \Theta_4(\theta)$$

where Θ_1 to Θ_4 can be any functions of θ . It follows from equation (37) that the boundary condition (32) will be satisfied if we put

$$\Theta_1 = -\frac{1}{2}(r_1^*)^2\Theta \quad (39)$$

Hence, equations (36), (37), and (39) show that

$$\left. \frac{\partial P^*}{\partial r^*} \right|_{r^*=1} = \frac{1}{2}\Theta(\theta)[1 - (r_1^*)^2] \quad (40)$$

Equations (36) and (38) show that condition (31) is satisfied if we set

$$p^*(\theta, z^*) = \Theta_5(\theta) + \Theta_3(\theta)z^* - \frac{1}{2}(z^*)^2\Theta(\theta) \quad (41)$$

where we have put

$$\Theta_5 = \frac{1}{4}\Theta + \Theta_2 + \Theta_4$$

The boundary condition (33a) will be satisfied if we choose the functions Θ_3 and Θ_5 of θ in equation (41) so that

$$p^*(\theta, z^*) = -\frac{1}{2}\Theta(\theta) \left[(z^*)^2 - \left(\frac{l^*}{2} \right)^2 \right] \quad (42)$$

Finally, it follows from equations (40) and (42) that equation (34) will be satisfied if we choose the function Θ so that

$$\Theta(\theta) = \frac{-\frac{d}{d\theta} [h^*(1 + \Xi_0)]}{[(h^*)^3(1 + \Xi_1) + 12\Psi_0]} \quad (43)$$

where we have put

$$\Psi_0 = \frac{1}{2}[(r_1^*)^2 - 1]\Psi = \frac{\kappa}{c^3} \frac{(r_1^2 - r_0^2)}{2r_0}$$

Hence, the differential equation and boundary conditions are all satisfied and we find from equations (26), (29), (42), and (43) that the pressure in the film region is given by

$$p^*(\theta, z^*) = \left[1 + \left(\frac{s}{1 + s + \epsilon \cos \theta} \right)^2 \right] \frac{\sin \theta \left[\left(\frac{l^*}{2} \right)^2 - (z^*)^2 \right]}{(1 + \epsilon \cos \theta)^3 [1 + \Xi_1(\theta)] + 12\Psi_0} \quad (44)$$

The pressure distribution within the porous region itself is of little interest and we shall therefore not write out an expression for it explicitly. Thus, the solution to the porous bearing problem in the short-bearing limit is given by equation (44). This result, of course, reduces to the equation obtained in reference 2 when s is put equal to zero. Having obtained an expression for the pressure distribution in the film, it is now necessary to use this result to calculate the quantities of principal interest. The first of these is the load supported by the bearing.

Load on short bearing. - We shall now find expressions for the magnitude and direction of the external load which will equilibrate the pressure generated in the film. The X and Y axis are as shown in figure 3. The components of the load are obtained by integrating the component of the pressure force over the surface of the bearing. In calculating the loads on short porous bearings it has always been assumed in previous analyses that the half-Sommerfeld condition is appropriate (refs. 2, and 4 to 6). We shall also follow this procedure. Thus, it is assumed that the pressure distribution for $0 \leq \theta \leq \pi$ is given by equation (44) and the pressure is put equal to zero for $\pi < \theta \leq 2\pi$. When this condition is used, the X and Y components of the load W_X and W_Y are

$$\left. \begin{aligned} W_X &= \int_{-l/2}^{l/2} \int_0^\pi p r_0 \cos \theta \, d\theta \, dz \\ W_Y &= \int_{-l/2}^{l/2} \int_0^\pi p r_0 \sin \theta \, d\theta \, dz \end{aligned} \right\} \quad (45)$$

Or upon defining the dimensionless load components W_X^* and W_Y^* by

$$W_X^* = \frac{W_X}{u_s \eta} \left(\frac{c}{l} \right)^2$$

$$W_Y^* = \frac{W_Y}{u_s \eta} \left(\frac{c}{l} \right)^2$$

equations (45) become

$$W_X^* = \frac{6}{(l^*)^3} \int_{-l^*/2}^{l^*/2} \int_0^\pi p^* \cos \theta \, d\theta \, dz^*$$

$$W_Y^* = \frac{6}{(l^*)^3} \int_{-l^*/2}^{l^*/2} \int_0^\pi p^* \sin \theta \, d\theta \, dz^*$$

Upon inserting equation (44) into these expressions and performing the integration with respect to z^* we get

$$\left. \begin{aligned} W_X^* &= \frac{\epsilon}{2} \int_0^\pi \left[1 + \left(\frac{s}{1+s+\epsilon \cos \theta} \right)^2 \right] \frac{\sin \theta \cos \theta}{(1+\epsilon \cos \theta)^3 [1 + E_1(\theta)] + 12\Psi_0} \, d\theta \\ W_Y^* &= \frac{\epsilon}{2} \int_0^\pi \left[1 + \left(\frac{s}{1+s+\epsilon \cos \theta} \right)^2 \right] \frac{\sin^2 \theta}{(1+\epsilon \cos \theta)^3 [1 + E_1(\theta)] + 12\Psi_0} \, d\theta \end{aligned} \right\} \quad (46)$$

The magnitude W of the load on the bearing is

$$W = \sqrt{W_X^2 + W_Y^2}$$

and the Sommerfeld number Δ is

$$\Delta = \frac{W}{u_s \eta} \left(\frac{c}{r_0} \right)^2 \quad (47)$$

Hence

$$\Delta \left(\frac{r_0}{l} \right)^2 = \sqrt{(W_X^*)^2 + (W_Y^*)^2} \quad (48)$$

The attitude angle ψ shown in figure 3 is defined by

$$\tan \psi = \frac{W_Y}{-W_X}$$

or

$$\psi = \tan^{-1} \left(\frac{W_Y^*}{-W_X^*} \right) \quad (49)$$

The other important quantity that must be calculated is the friction in the bearing.

Friction in short bearings. - The shear stress τ_h acting on the shaft for any porous bearing is given by equation (21a). However, as indicated in reference 16 (p. 85), it is consistent with the short-bearing approximation to neglect the circumferential pressure gradient term in this equation. Thus, in the short-bearing limit

$$\tau_h = \frac{\eta u_s}{h} (1 - \Xi_0)$$

The circumferential friction force F acting on the shaft is then

$$F = \int_{-l/2}^{l/2} \int_0^{2\pi r_0} \tau_h \, dz \, dx = \eta u_s \int_{-l/2}^{l/2} \int_0^{2\pi r_0} \frac{1}{h} (1 - \Xi_0) \, dz \, dx$$

Upon substituting equations (9), (16) and (29) this becomes

$$\frac{F}{l} = \frac{\eta r_0^u s}{c} \int_0^{2\pi} \frac{d\theta}{1 + s + \epsilon \cos \theta}$$

Performing the integration gives

$$\frac{F}{l} = \frac{2\pi \eta r_0^u s}{c} \frac{1}{\sqrt{(1+s)^2 - \epsilon^2}} \quad (50)$$

The coefficient of friction μ of the bearing is defined as the frictional force on the shaft divided by the total load supported by the bearing. Thus, upon using equation (47)

$$\mu \frac{r_0}{c} = \left(\frac{F}{W} \right) \left(\frac{r_0}{c} \right) = \frac{2\pi}{\Delta} \frac{1}{\sqrt{(1+s)^2 - \epsilon^2}} \quad (51)$$

RESULTS AND DISCUSSION

An analysis has been carried out to determine the effect of slip observed in references 13 and 14 on the performance of porous metal journal bearings. To simplify the results, the short-bearing approximation was used and the technique developed by Morgan and Cameron for the case with no slip was adapted to obtain approximate solutions. Expressions were obtained for the total load carried by the bearing, the attitude angle, and the coefficient of friction. Before discussing the numerical values of these quantities it will be helpful to get some idea of the numerical values of the parameters appearing in the solutions which correspond to the most frequently used porous bearings.

As indicated in reference 2 the majority of porous bearings have a porosity between 25 and 35 percent. In this reference a curve of permeability as a function of porosity is plotted for porous bronze, one of the most commonly used porous bearing materials. This curve (without graphite) shows that when the porosity is between 25 and 35 percent the permeability is between 10^{-9} and 2×10^{-9} square centimeter. Figure 24.7 on page 57 of reference 15 shows that for the smaller bearings (shaft diameter, 1 in. (2.5 cm) or less) the clearance is of the order of 10^{-3} centimeters. Using a value of α equal to 1/10 as given in reference 14 we see that a reasonable value for the parameter $s = \sqrt{\kappa}/\alpha c$ is between 0.25 and 0.5 for the smaller porous bearings. For a bearing

1 inch (2.5 cm) in diameter or less, a reasonable length (ref. 15, p. 305) is about 1/2 inch or 1 centimeter. Now, as pointed out by Pinkus in his discussion of reference 5, the thickness $r_1 - r_0$ is approximately one-tenth the length of the bearing. Hence, for a 1-inch (2.5 cm) shaft $r_1 - r_0$ is of the order of one-tenth of a centimeter. For $r_1 - r_0 \ll r_0$, the parameter Ψ_0 is approximately $(r_1 - r_0)\kappa/c^3$; or for the values given above, Ψ_0 is of the order of 1/10. Hence, for the smaller sizes of porous bearings (shaft diameters 1 inch (2.5) or less) reasonable values for the parameter s lie between 1/4 and 1/2 and the value of the parameter Ψ_0 is of the order of 1/10.

The total load carried by the porous bearing is given by equation (30) and equations (46) to (48) as a function of the parameters ϵ , Ψ_0 , s , and α . When s is put equal to zero, the solution with the slip neglected which was obtained in references 2 and 4 is recovered. The dimensionless load Δ is referred to as the Sommerfeld number and the dimensionless load $\Delta(r_0/l)^2$ is sometimes referred to as the Ocvirk number (ref. 5). The ocvirk number is plotted in figures 4 to 7 as a function of the permeability parameter Ψ_0 for various values of the eccentricity ratio ϵ . In each figure the curves for the no-slip case ($s = 0$) are shown dashed for comparison purposes. Curves are presented for the typical values of the slip parameter s of 0.5 and 0.25 determined previously. Values of α of 0.1 and 1 are used.

These figures show that increasing the permeability or the bearing thickness decreases the load-carrying capacity. The figures also show that for a given speed and eccentricity ratio the effect of increasing slip (measured by increasing s) is generally to decrease the load-carrying capacity. However, for high enough eccentricity ratios this effect is actually reversed and the slip actually results in a slight increase in load-carrying capacity over the case where no slip occurs.

In figure 8, the fractional error due to neglecting slip in the calculations is plotted as a function of eccentricity ratio for the typical values of the parameters for small, high-speed, low-load bearings which were stated previously. This figure shows that the error incurred can be as much as 30 percent.

The attitude angle ψ (see fig. 3) is calculated from equations (30), (46), and (49). The results of these calculations (for the same ranges of parameters as used for the load) are shown as a function Ψ_0 in figures 9 to 11. The results show that the attitude angle increases with increasing permeability parameter Ψ_0 and decreasing eccentricity ratio ϵ . The figures also show that for low values of Ψ_0 the effect of slip is to increase the attitude angle slightly, whereas for high values of Ψ_0 the effect of slip is to decrease the attitude angle slightly. In any case the slip has only a relatively small effect on the attitude angle.

The coefficient of friction of the bearing is given by equation (51). It is shown in reference 15 (p. 551) that, if the effects of slip are neglected, the formula for the coefficient of friction is the same for porous bearings as it is for nonporous bearings:

namely,

$$\mu\left(\frac{r_0}{c}\right) = \frac{2\pi}{(1 - \epsilon^2)^{1/2} \Delta}$$

Thus, the effects of slip can be taken into account by replacing the term $(1 - \epsilon^2)^{1/2}$ in this formula by the term $[(1 + s)^2 - \epsilon^2]^{1/2}$. This does not mean, however, that the slip always reduces the coefficient of friction, since, other things being equal, the slip will in most cases reduce Δ . The effect of slip on the coefficient of friction can be calculated by using equations (30), (46), (48), and (51). The results of these calculations are shown in figures 12 and 13. It can be seen from these figures that increasing the porosity parameter Ψ_0 or decreasing the eccentricity ratio ϵ increases the coefficient of friction. Also the effect of slip is to decrease the coefficient of friction at large values of Ψ_0 and to increase the coefficient of friction at small values of Ψ_0 . In figure 14 the fractional error due to neglecting slip in calculating the coefficient of friction is plotted as a function of eccentricity ratio for the typical value of the parameters for small, high-speed, light-load bearings obtained above (curve with $\Psi_0 = 0.1$). Also shown in the figure is a curve corresponding to larger sized bearings (curve with $\Psi_0 = 1$). This figure shows that for the higher eccentricity ratios very large errors in the predicted value of the coefficient of friction will result if the effects of slip are neglected. For $\Psi_0 \geq 1$ the factor Δ in equation (51) is relatively unaffected by the slip. Hence, the reduction in the coefficient of friction is due almost entirely to the term $\sqrt{(1 + s)^2 - \epsilon^2}$. This shows that the curve drawn for $\Psi_0 = 1$ in figure 14 also applies for all values of Ψ_0 larger than 1 and that the results obtained with slip neglected with $\Psi_0 > 1$ merely need be corrected by the factor $(1 - \epsilon^2)^{1/2} / [(1 + s)^2 - \epsilon^2]^{1/2}$.

CONCLUDING REMARKS

An analysis has been performed to determine the effects of slip at a porous surface on the performance of porous metal bearings. Other things being equal, the slip effects usually reduce both the load-carrying capability and the coefficient of friction of the bearing. For the larger eccentricity ratio this reduction in the coefficient of friction can be very large. However, the slip has little effect on attitude angle.

Lewis Research Center,
National Aeronautics and Space Administration,
Cleveland, Ohio, October 29, 1970,
129-01.

APPENDIX - SYMBOLS

c	concentric clearance	u_s	surface speed of shaft
e	eccentricity	V_r	radial component of Darcy velocity
F	friction force on shaft	V_θ	azimuthal component of Darcy velocity
f	function defined on p. 7	V_z	axial component of Darcy velocity
g	function defined on p. 7	v	z-component of velocity in film
h	film thickness	W	total load supported by bearing
h^*	h/c	W_X	X-component of load supported by bearing
l	length of bearing	W_Y	Y-component of load supported by bearing
l^*	l/r_0	W_X^*	$\frac{W_X/l}{u_s \eta} \left(\frac{c}{l}\right)^2$
P	pressure within porous bearing (above ambient)	W_Y^*	$\frac{W_Y/l}{u_s \eta} \left(\frac{c}{l}\right)^2$
P^*	$Pc^2/6u_s \eta r_0$	w	y-component of velocity in film
p	pressure within film (above ambient)	X	coordinate for external load
p^*	$pc^2/6u_s \eta r_0$	x	coordinate for film
\bar{Q}	Darcy velocity in porous bearing	Y	coordinate for external load
q_x	x-component of integrated volume flux	y	coordinate for film
q_y	y-component of integrated volume flux	y^*	y/r_0
R	defined by eq. (36)	Z	defined by eq. (36)
r	radial coordinate	z	axial coordinate for film and interior or porous bearing
r_0	inner radius of porous bearing	z^*	z/r_0
r_1	outer radius of porous bearing	α	slip coefficient
r^*	r/r_0	Δ	Sommerfeld number, $\frac{W/l}{u_s \eta} \left(\frac{c}{r_0}\right)^2$
r_1^*	r_1/r_0		
s	slip parameter $\sqrt{k}/\alpha c$		
u	x-component of velocity in film		

ϵ	eccentricity ratio, e/c
η	absolute viscosity
$\Theta, \Theta_1,$ Θ_2, \dots	function of θ
θ	azimuthal coordinate
κ	permeability of bearing material
Ξ_0, Ξ_1	functions defined by equations (29) and (30)
μ	coefficient of friction, F/W
τ_h	shear stress on shaft
τ_0	shear stress on bearings
Ψ	$\kappa r_0/c^3$
Ψ_0	porosity parameter, $\frac{\kappa}{c^3} \frac{(r_1^2 - r_0^2)}{2r_0}$
ψ	attitude angle

REFERENCES

1. Booser, E. R.: Plain-Bearing Materials. *Machine Design*, vol. 42, June 18, 1970, pp. 14-20.
2. Morgan, V. T.; and Cameron, A.: Mechanism of Lubrication in Porous Metal Bearings. *Proceedings of the Conference on Lubrication and Wear*. Inst. Mech. Eng., London, 1957, pp. 151-157.
3. Ocvirk, R. W.: Short-Bearing Approximation for Full Journal Bearings. NACA TN 2808, 1952.
4. Rouleau, Wilfred T.: A Note on the Lubrication of Porous Metal Bearings. *J. Basic Eng.*, vol. 84, no. 1, Mar. 1962, pp. 205-206.
5. Rouleau, W. T.: Hydrodynamic Lubrication of Narrow Press-Fitted Porous Metal Bearings. *J. Basic Eng.*, vol. 85, no. 1, Mar. 1963, pp. 123-128.
6. Rhodes, C. A.; and Rouleau, W. T.: Hydrodynamic Lubrication of Narrow Porous Metal Bearings With Sealed Ends. *WEAR*, vol. 8, 1965, pp. 474-486.
7. Shir, C. C.; and Joseph, D. D.: Lubrication of a Porous Bearing - Reynolds' Solution. *J. Appl. Mech.*, vol. 33, no. 4, Dec. 1966, pp. 761-767.
8. Joseph, D. D.; and Tao, L. N.: Lubrication of a Porous Bearing - Stokes' Solution. *J. Appl. Mech.*, vol. 33, no. 4, Dec. 1966, pp. 753-760.
9. Rhodes, C. A.; and Rouleau, W. T.: Hydrodynamic Lubrication of Partial Porous Metal Bearings. *J. Basic Eng.*, vol. 88, no. 1, Mar. 1966, pp. 53-60.
10. Sneck, H. J.; and Yen, K. T.: The Externally Pressurized, Porous Wall, Gas-Lubricated Journal Bearing. I. *ASLE Trans.*, vol. 7, no. 3, July 1964, pp. 288-298.
11. Sneck, H. J.; and Elwell, R. C.: The Externally Pressurized, Porous Wall, Gas-Lubricated Journal Bearing. II. *ASLE Trans.*, vol. 8, no. 4, Oct. 1965, pp. 339-345.
12. Sneck, H. J.; and Yen, K. T.: The Externally Pressurized, Porous Wall, Gas-Lubricated Journal Bearing-III. *ASLE Trans.*, vol. 10, no. 3, July 1967, pp. 339-347.
13. Beavers, Gordon S.; and Joseph, Daniel D.: Boundary Conditions at a Naturally Permeable Wall. *J. Fluid Mech.*, vol. 30, Oct. 17, 1967, pp. 197-207.
14. Beavers, G. S.; Sparrow, E. M.; and Magnuson, R. A.: Experiments on Coupled Parallel Flows in a Channel and a Bounding Porous Medium. Paper 70-FE-11, ASME, May 1970.

15. Cameron, A.: *The Principles of Lubrication*. John Wiley & Sons, Inc., 1966.
16. Bisson, Edmond E.; and Anderson, William J.: *Advanced Bearing Technology*. NASA SP-38, 1964.

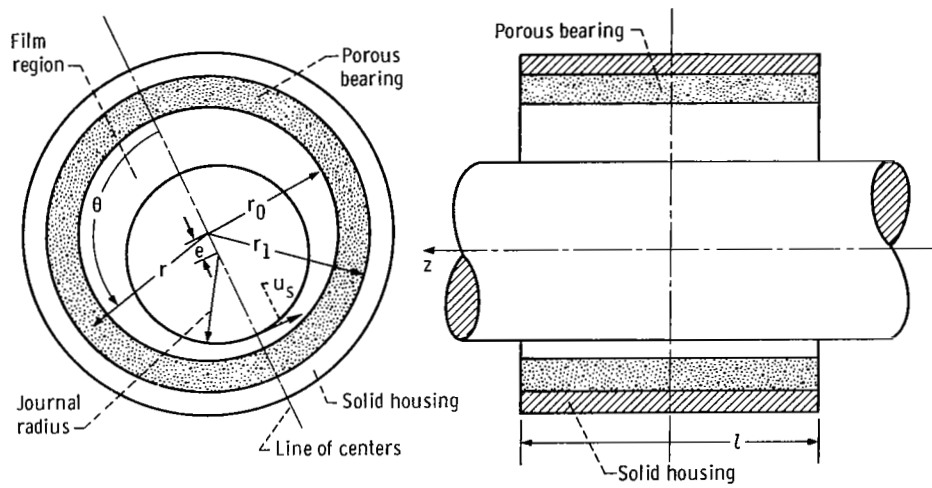


Figure 1. - Porous bearing configuration.

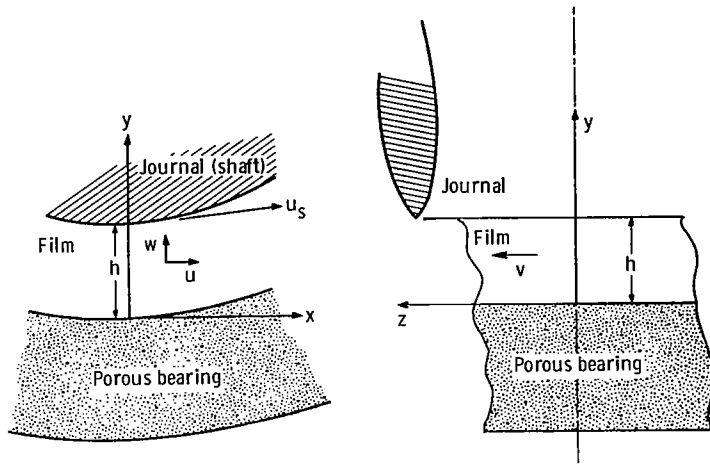


Figure 2. - Coordinate system for film region.

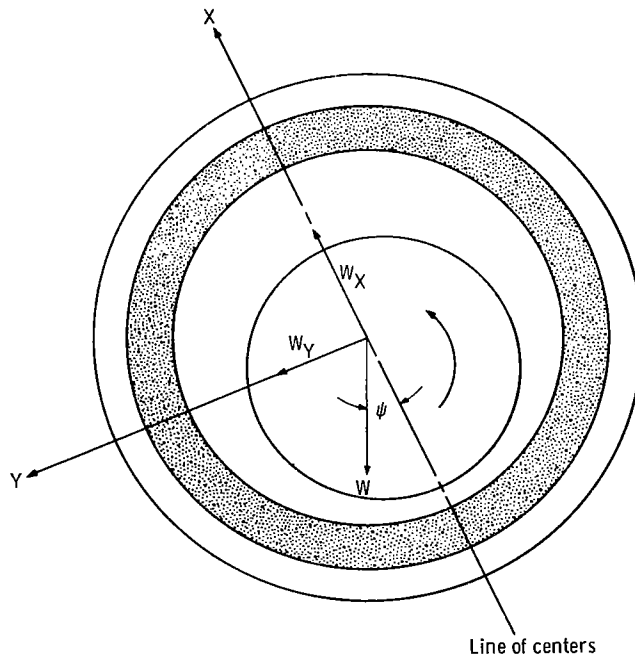


Figure 3. - Configuration for load components.

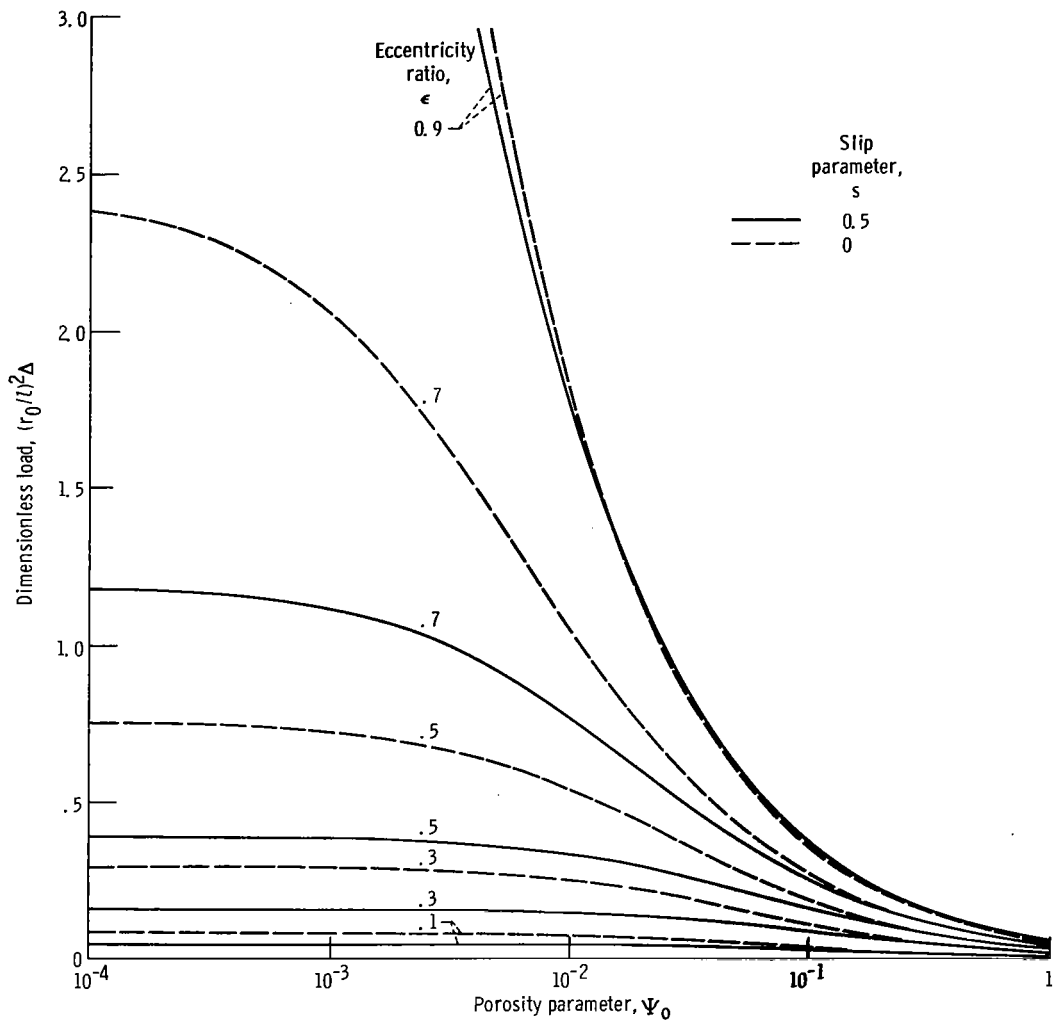


Figure 4. - Bearing load at slip coefficient of 0.1 and slip parameter of 0.5.

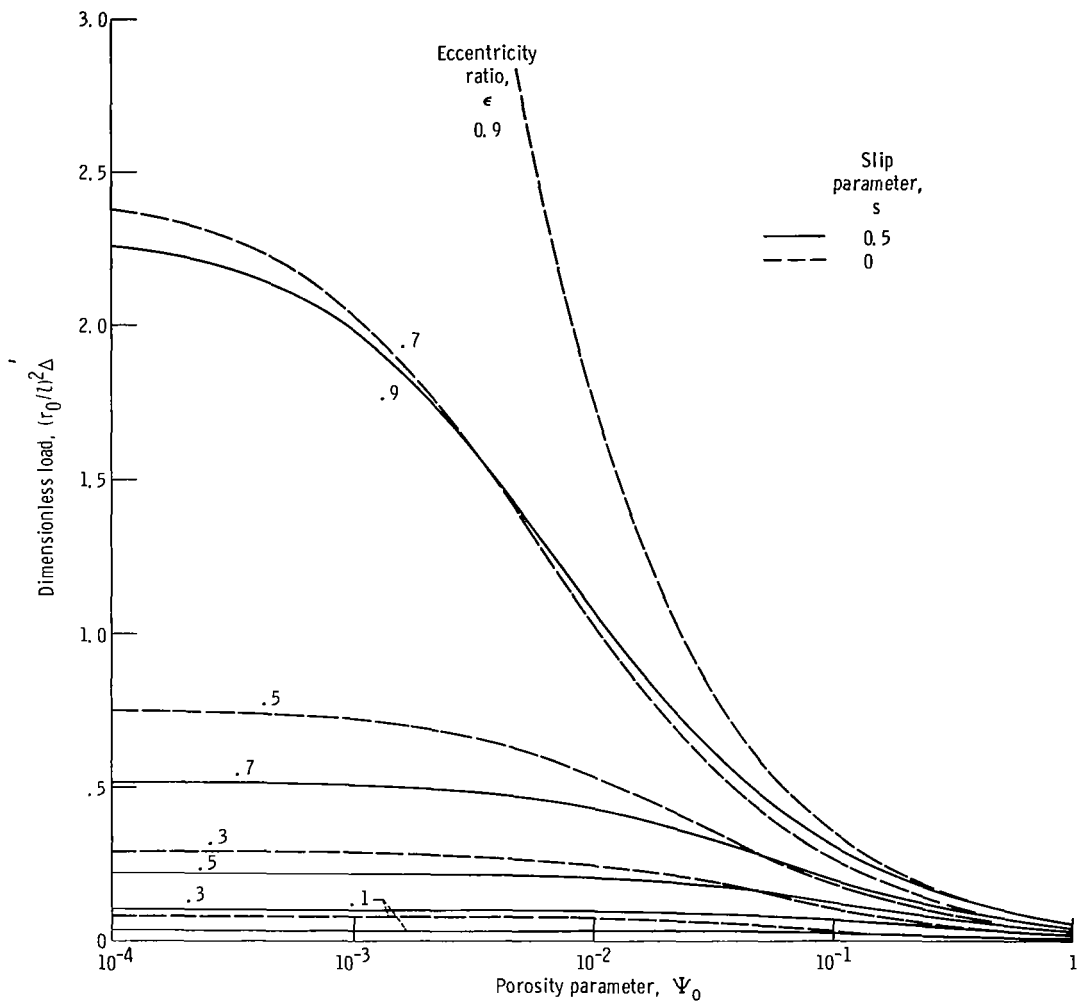


Figure 5. - Bearing load at slip coefficient of 1.0 and slip parameter of 0.5.

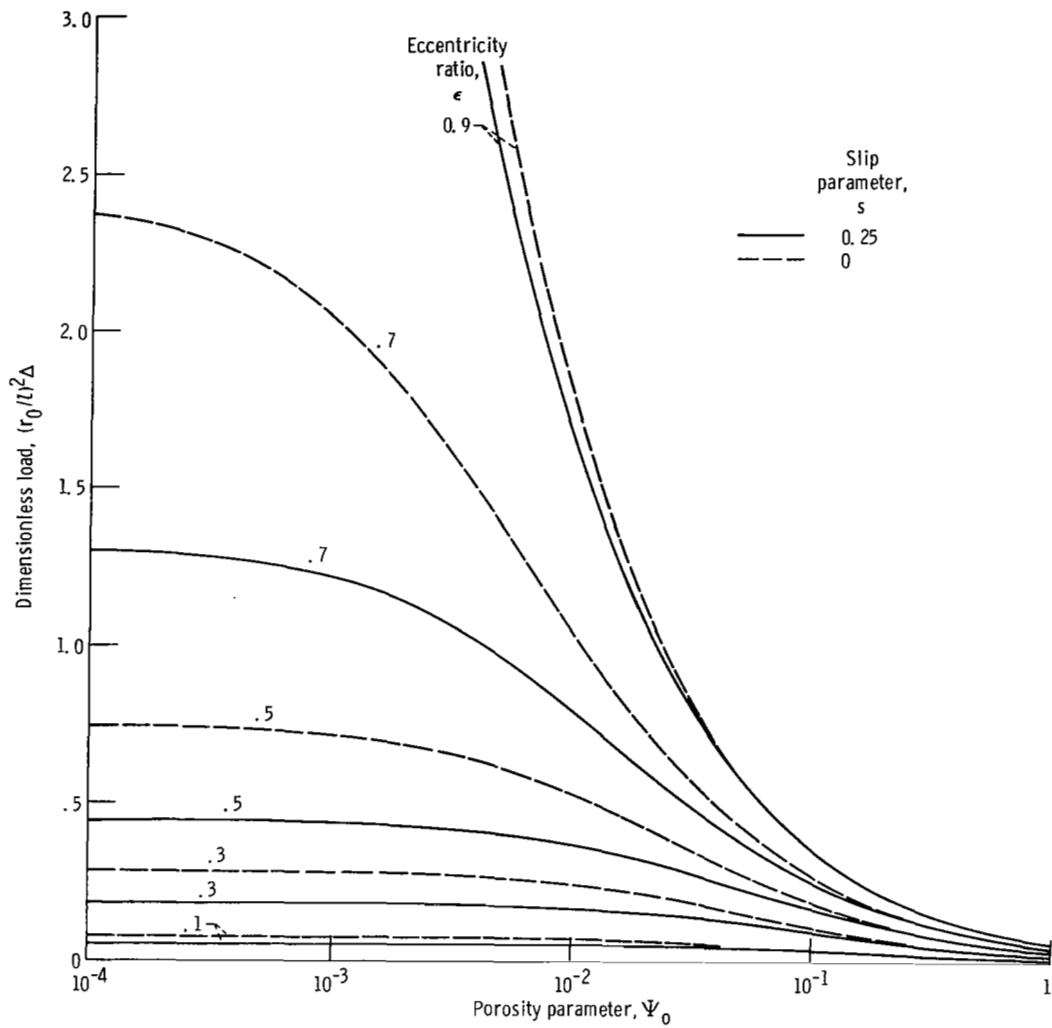


Figure 6. - Bearing load at slip coefficient of 0.1 and slip parameter of 0.25.

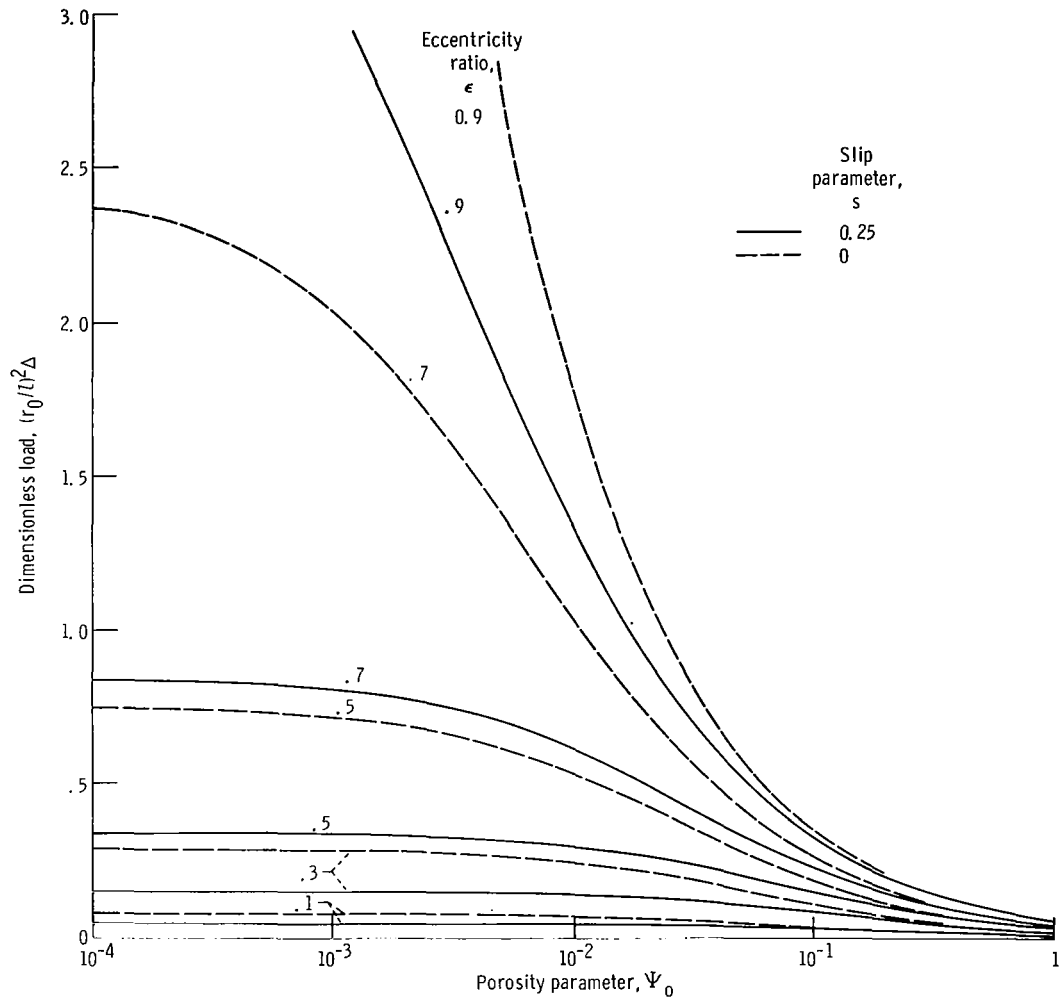


Figure 7. - Bearing load at slip coefficient of 1.0 and slip parameter of 0.25.

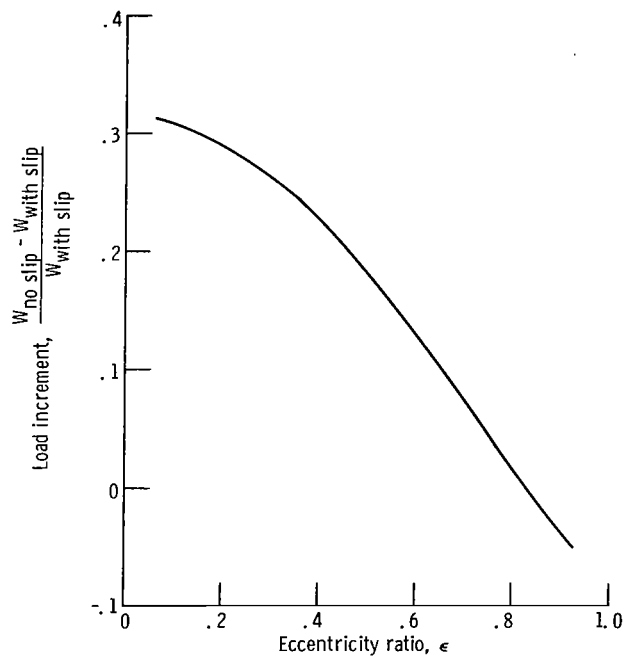


Figure 8. - Fractional error in load due to no-slip condition. Porosity parameter, 0.1; slip coefficient, 0.1; slip parameter, 0.5.

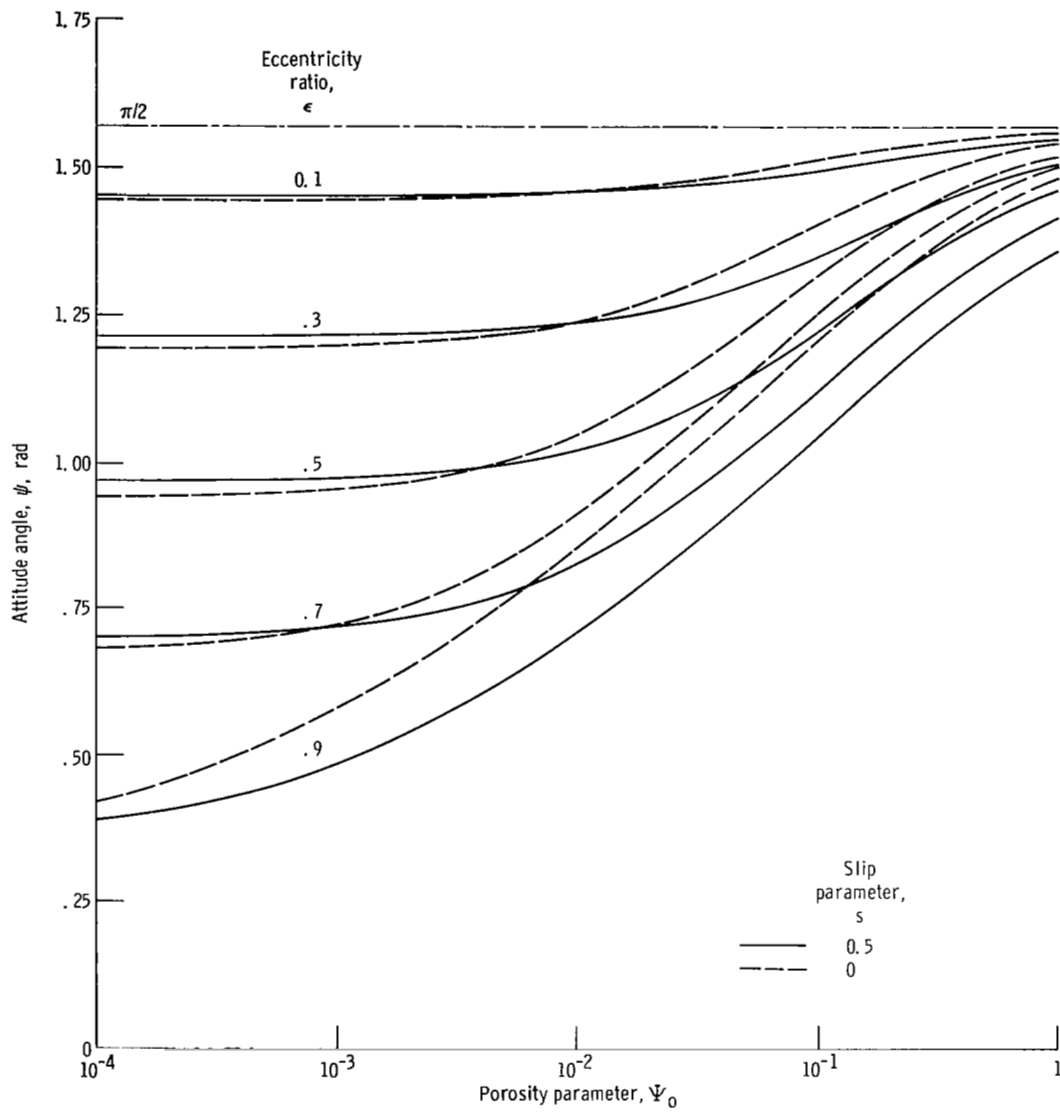


Figure 9. - Attitude angle at slip coefficient of 0.1 and slip parameter of 0.5.

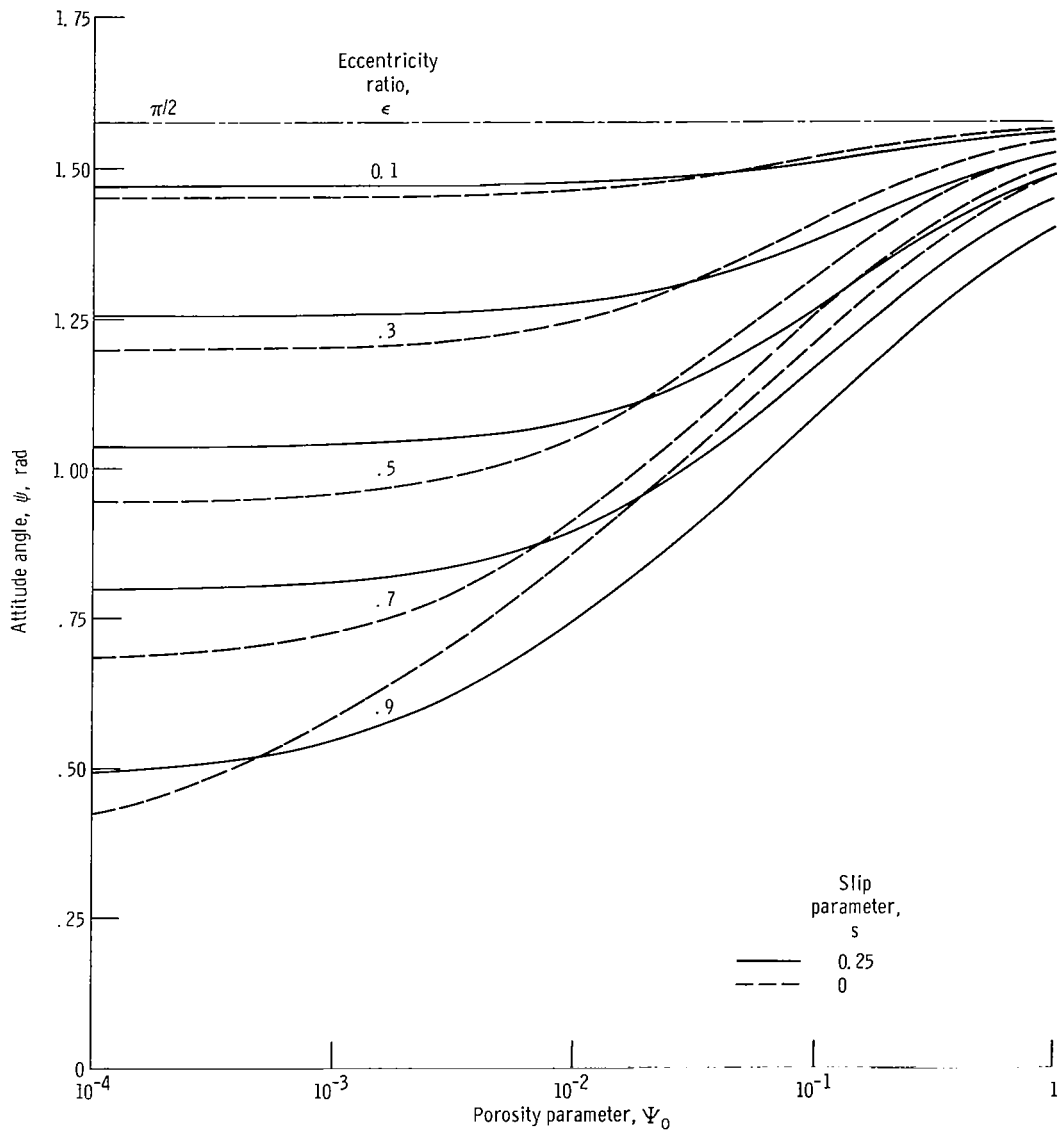


Figure 10. - Altitude angle at slip coefficient of 1.0 and slip parameter of 0.25.

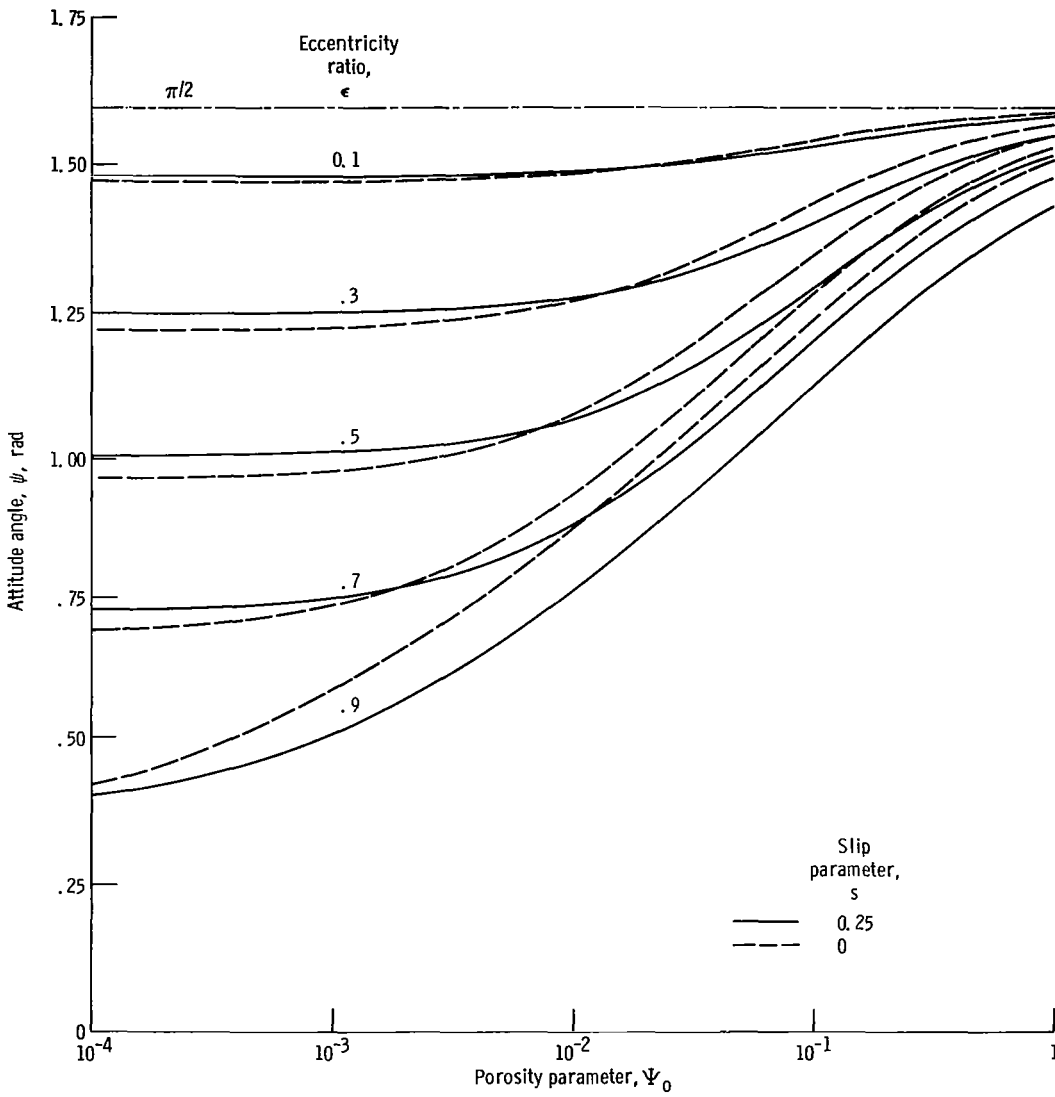


Figure 11. - Attitude angle at slip coefficient of 0.1 and slip parameter of 0.25.

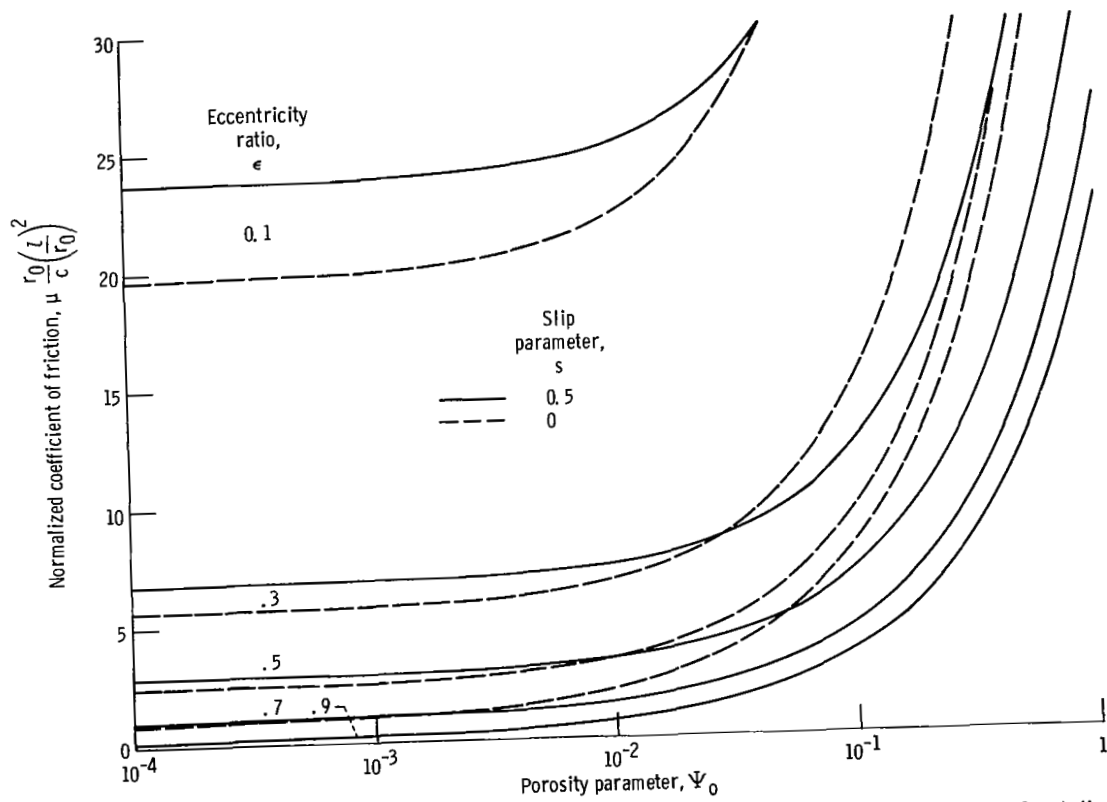


Figure 12. - Normalized coefficient of friction as function of porosity parameter for slip coefficient of 0.1 and slip parameter of 0.5.

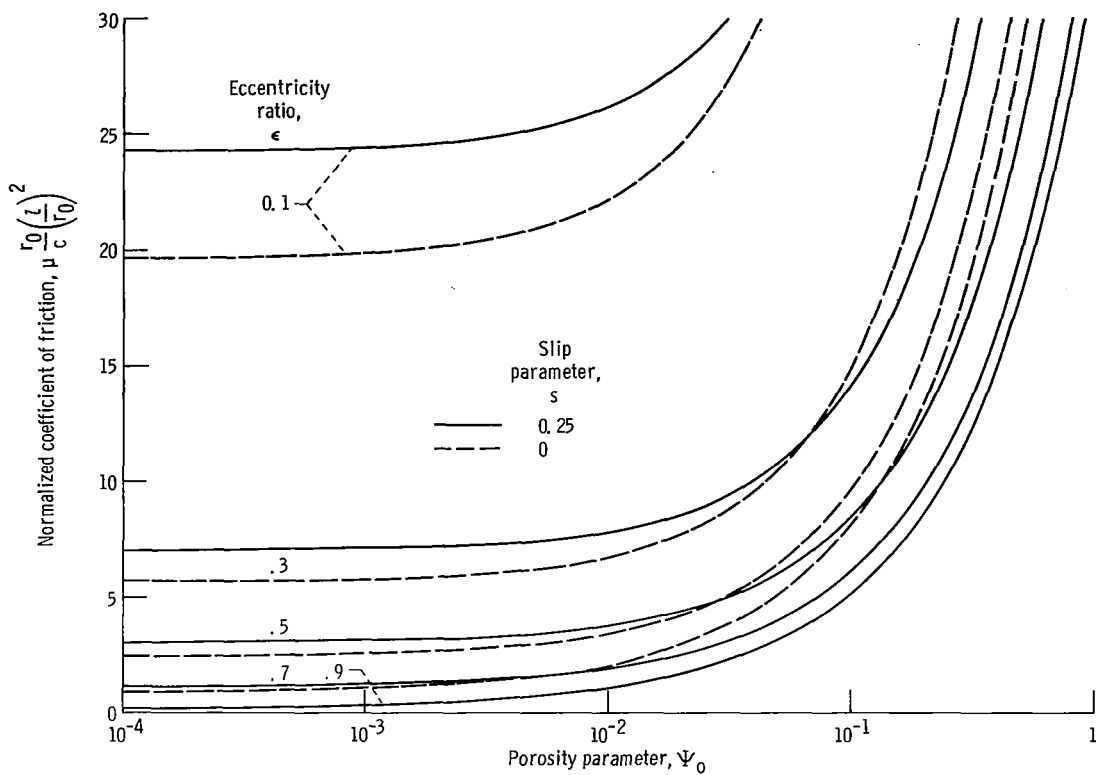


Figure 13. - Normalized coefficient of friction as function of porosity parameter for slip coefficient of 0.1 and slip parameter of 0.25.

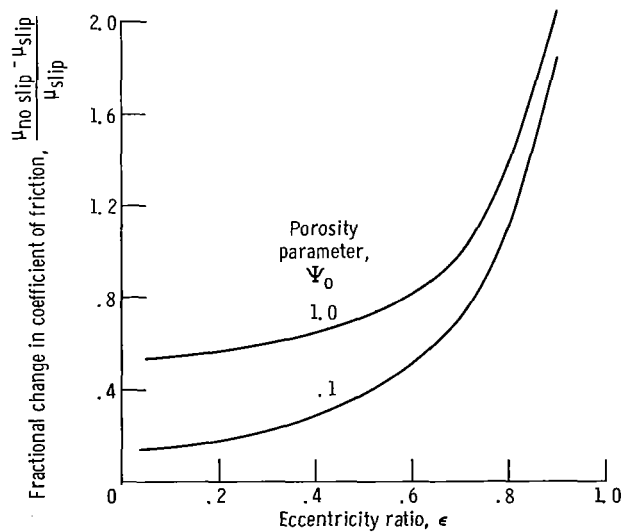


Figure 14. - Error in normalized coefficient of friction due to no-slip condition, at slip coefficient of 0.1 and slip parameter of 0.5.